Synthesis, Characterization and Mechanical Properties of Alumina-Zirconia Nanocomposite Particles

Ramzan Muhammad[1], Bimlesh Kumar[2], Atul Chaskar[3]

[1]*MMANTC, Malegaon; 3158, Lane No.1, Akbar Chawk, Dhule-424001 (M.S.) India*
[2] *Department of Mechanical Engineering, Sant Gajanan College of Engineering, Kolhapur*
[3]*Department of Dyestuff Technology, Institute of Chemical Technology, Matunga, Mumbai*

Abstract: *Ceramic nanocomposites have attracted a great interest of recent researchers due to its excellent attributes suitable for industrial applications such as tool engineering. In this study alumina-zirconia (Al_2O_3-ZrO_2) nanocomposite particles are prepared by sol-gel synthesis route and mechanical properties are determined using Halpin-Tsai approach. SEM and TEM images clearly indicate the nanosize of composite particles and dispersion of ZrO_2 in Al_2O_3 matrix. The results of micrographs are in close agreement with FTIR and XRD spectra. The microstructural modification in the precursor to form the nanocomposite ceramic is suggested in the detailed discussion. A MATLAB script is written to evaluate the physical and mechanical characteristics and it is predicted that tensile strength, flexural strength and Poisson's ratio of alumina can be enhanced excellently with reinforcement of zirconia. However hardness, elastic and shear modulii can decrease proportionately.*

Keywords: *Alumina, Mechanical properties, Nano composites, Sol-gel methods, Transmission electron microscopy (TEM)*

I. Introduction

During last decades, a considerable attention was focused on nanocomposites. A nanocomposite material will be formed that posses some unique properties both of the nanoparticles and the matrix where at least one of the dimensions of the filler material is of the order of a nanometer [1]. The ceramic matrix nanocomposites, which involve a uniform dispersion of nanometer size second phase particles, are a class of special materials, widely used for engineering applications [2-5]. Aluminum oxide is distinct in some properties such as high hardness, low coefficient of friction, high resistance to corrosion and thermodynamic stability ($\approx$ 1500-1700^{0}C) [6]. Thirunavukkarasu et al. [7] have discussed that the composite alumina - zirconia nanopowders were synthesized by sol gel process using the organometallic precursors such as aluminum secondary butoxide and zirconium n-propoxide. Zirconia (ZrO_2) which has been utilized for transformation toughening to synthesize several composites like ZrO_2-TiB_2, WC-ZrO_2, Al_2O_3-ZrO_2, Mullite-ZrO_2, Si_3N_4-ZrO_2, Intermetallic (Fe-Al)-ZrO_2 etc. [8-10]. Among these composites, Zirconia Toughened Alumina (ZTA) ceramics have received a significant scientific and technological attention during the last two decades for industrial applications such as cutting tools, dye or prosthesis components because of their excellent room temperature strength, toughness and wear resistance. The lowest wear rate ($10^{-9}mm^3$/Nm) for ZTA against TZP (Tetragonal Zirconia Polycrystals) was reported by Kerkwijk et al.[11]. Enomoto [12] prepared Al_2O_3-ZrO_2 composite through wet-chemical process in which t-ZrO_2 particles of ~30nm were finely dispersed within the alumina grains. ZTA ceramics were also conventionally prepared by Tang et al. [13, 14] through 0–15-vol% ZrO_2, using two processing methods: powder mixing and a modified colloidal route. Microstructure and mechanical properties of ZTA fabricated by liquid phase sintering with addition of 1 wt% TiO_2, 1 wt. % MnO_2 and 2wt. % CaO–Al_2O_3–SiO_2 (CAS) as sintering aids was studied by Huang et al. [15]. Casellas et al. [16] described the microstructure coarsening in ZTA on the basis of systems formed by second phase, which increased the fracture toughness and decreased the hardness of the synthesized material. Quintina et al. [17] have shown that the sol-gel processing method of ZTA results in a better control over microstructure than the powder based process and materials with good mechanical properties with a better control of porosity can be produced. Dakskobler and Kosmac [18] have prepared the alumina-zirconia composites from viscous non-polar suspensions of alumina and zirconia powders in which flexural strength increased due to the strengthening effect of the zirconia phase for layer microstructure refinement. Aruna and Rajam [19] used solution combustion synthesis and obtained less than 10nm ZTA particle, which was controlled by the proper fuel ratio and the energetic of the combustion reaction. In this study zirconia toughened alumina nanocomposite particles are synthesized through sol-gel processing route. The process is found to be excellent in controlling the particle size, distribution and structural morphology illustrated by TEM and SEM images. FTIR and XRD spectra are in close agreement with micrograph results. The mechanical and physical properties of nanocomposite particles are evaluated by using

---

Halpin-Tsai approach. A perspective visualization in accordance with microscopic structural modification is suggested in detailed discussion.

II. Experimentation

Alumina-zirconia (Al_2O_3-ZrO_2) nanocomposite particles were synthesized through sol-gel method with a minor modification in the protocol as reported by Sarkar et al. [20]. Hydrated $Al(NO_3)_3.9H_2O$ and $ZrOCl_2.8H_2O$ (Both from Loba Chemie, India) were used as precursor. The requisite amounts of precursor were mixed with distilled water to achieve the solution gelation. The mixed hydrogel was obtained by adding 1:1 NH_3 solution into the mixed aqueous solution maintained at ambient temperature (27°C) with continuous stirring by magnetic stirrer. As NH_3 solution is added dropwise the viscosity of the solution gradually increases and finally set to an enblock gel at pH 8.7. The gel was washed with boiling distilled water and filtered repeatedly after aging for 24 hours to remove chloride and nitrate ions. The dried gel was calcined in muffle furnace at 900^0C in still air for 4 hours soaking time. Acetone washing was carried out to deagglomerate the nanoparticles after calcination. The complete process is illustrated by the flow chart show in Fig. 1. The SEM, TEM and FTIR are conducted at SAIF, IIT Bombay, Mumbai and XRD is carried out at UICT, NMU, Jalgaon. The TEM was Philips make, model CM200, Operating voltage 200kv and Resolution 2.4A^o and SEM model was JSM-7600F, accelerating voltage 30 kV and resolution 1.0nm.

```
   ┌─────────────────────┐          ┌─────────────────────┐
   │ 95M, Al (NO₃)₃ 9H₂O │          │  5M, ZrOCl₂ 8H₂O    │
   └─────────────────────┘          └─────────────────────┘
                                          ┌──────────────┐
                                    ◄─────│ 1:1 NH₃ Solⁿ │
                                          └──────────────┘
                   ┌─────────────────────┐
                   │  Stirring till pH 8.7 │
                   └─────────────────────┘
                   ┌───────────────────────────┐
                   │  Aging at Room Temp (24 Hrs) │
                   └───────────────────────────┘
                   ┌──────────────────────────────────┐
                   │ Hot water washing till Cl & NO₃ free │
                   └──────────────────────────────────┘
                   ┌──────────────────────────┐
                   │  Drying at 40⁰C (48 Hrs)  │
                   └──────────────────────────┘
                   ┌──────────────────────────┐
                   │ Calcination at 900⁰C (4 Hrs) │
                   └──────────────────────────┘
                   ┌──────────────────────┐
                   │   Acetone washing     │
                   └──────────────────────┘
                   ┌──────────────────────┐
                   │   Drying at 50⁰C      │
                   └──────────────────────┘
                   ┌──────────────────────────┐
                   │  Al₂O₃-ZrO₂ Nanopowders  │
                   └──────────────────────────┘
```
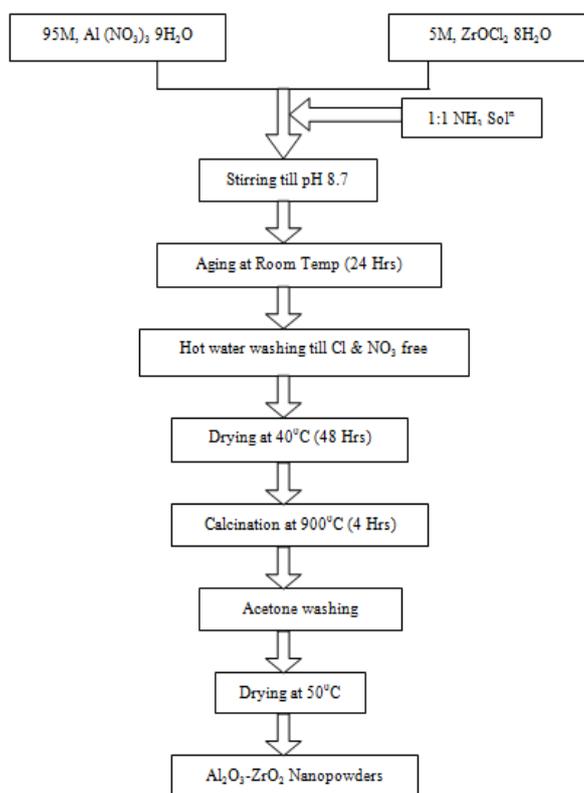
Fig. 1. Flowchart of sol-gel synthesis to prepare Al_2O_3-ZrO_2 nanocomposite particles.

III. Results And Discussion

3.1 Transmission electron microscopy (TEM)

TEM micrographs clearly exhibit the microstructural morphology of nanocomposite and well dispersed zirconia nanoparticles in the alumina matrix. Shape of the particles is not exactly spherical due to agglomeration during calcinations at 900^0C. The dark spots inside the grey matrix indicate tetragonal-zirconia in the orthorhombic-alumina matrix which is amorphous in nature as validated also by x-ray diffractometry and FTIR spectra. The average particle size of Al_2O_3 is 49.78nm and that for reinforced ZrO_2 is 5.99nm. The surface morphology of the nanocomposite can be observed from the micrograph shown in Fig. 2. An approximation regarding the elemental composition (Al_2O_3-95% and ZrO_2 5%) of the composite can be established by observing the relative amount of grayish and dark region in the picture. Grey area shows alumina matrix whereas dark spots indicates zirconia fillers.
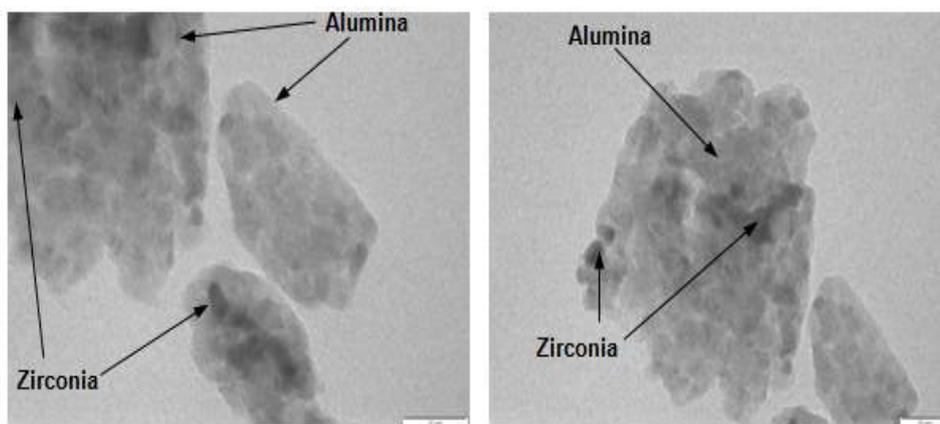
Fig. 2. TEM images of nanocomposite particles with 5% ZrO_2 in Al_2O_3 matrix.

3.2 Scanning electron microscopy (SEM)

SEM images in Fig. 3 show the surface morphology of the nanocomposite particles. Large specific surface area and high surface energy causes clustering of some nanoparticles. The aggregation may also be occurred probably due to atmospheric moisture after the process of drying. The uniformity of the particle at nanosize is a major advantage of sol-gel synthesis process. The uniform size attributes to uniformity of the physical and mechanical properties and isotropy of the particulate.
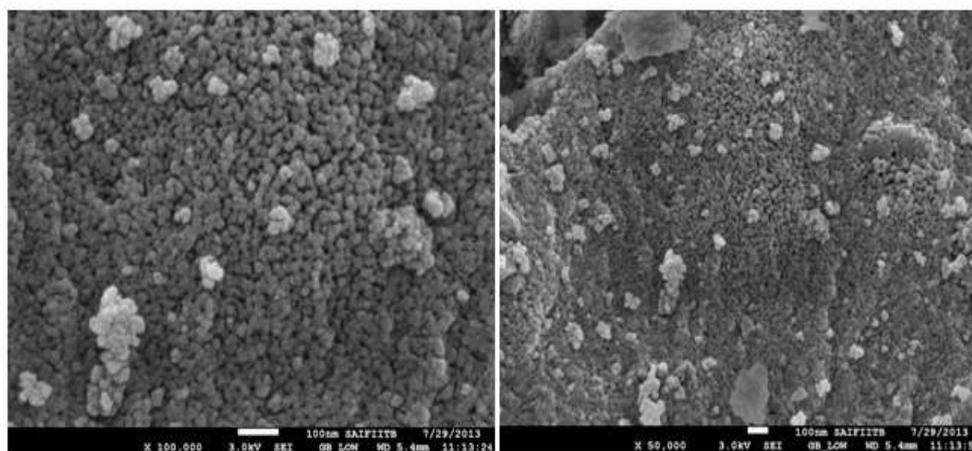
Fig. 3. SEM images of nanocomposite particles with 5% ZrO2 in Al2O3 matrix.

3.3 Fourier transform infra-red spectroscopy (FTIR)

Fig. 4 illustrates the FTIR spectrograph of the nanocomposite particles. IR Spectroscopy is an extremely effective method for determining the presence or absence of a wide variety of functional groups in a molecule. The peak at 529.67 cm^{-1} is the characteristic absorption of ZrO_2 and the broad absorption peaks at 3439.84 and 1632.13 cm^{-1} can be attributed to the characteristic absorption of Zr-OH (hydroxyls) group. The vibrations appearing in the range 4000 and 3000 cm^{-1} could be assigned to the coupling effect of stretching and bending vibrations of –OH groups. The bands at 711, 821.87 and 3786.72 cm^{-1} in the spectrum indicates the existence of ZrO_2 (hydroxyl group) which can be ascribed to the characteristic peaks of Al-O and Zr-O symmetric and asymmetric stretching vibrations. The strong absorption band of the FTIR spectrum may be attributed to six-coordinated Al^{3+} ions. The introduction of Zr^{4+} increases the cationic charge in the Al_2O_3-ZrO_2 composite which strongly interacts with the inner polar hydroxyl groups. This interaction creates an antisymmetric coupling force of attraction which probably results in the reduction of vibrational dipole moment in bending. Such results indicate that the active groups have been introduced into the matrix nanoparticle. These bands prove that ZrO_2 have been chemically bonded to the nano Al_2O_3 during the sol-gel processing. FTIR spectrum also illustrates that a trace of –OH group always remains in the structure of ZrO_2 reinforced Al_2O_3 nanocomposite even after heating at 900^0C which could also be due to the atmospheric moisture absorption.
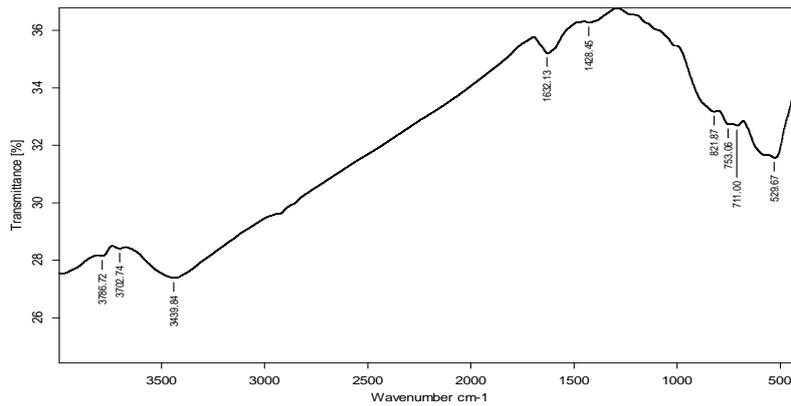
Fig. 4. FTIR spectrum of Al_2O_3-ZrO_2 nanocomposite.

3.4 X-ray diffractometry (XRD)

The XRD spectrum shown in Fig. 5 reveals that the alumina belongs to ҟAl_2O_3 space group pna21 (33) which is most suited for wear resistance coating on cemented carbide cutting tools. A series of characteristic peaks are observed as 300, 37, 116.26, 34.6 and 59.8 in accordance with the results of the previous researchers [21, 22]. The peaks shown in red are due to ZrO_2 and that in blue reflects the appearance of ternary oxides of Al_2O_3 matrix. The additional broad and high peaks in the spectrum due to ZrO_2 is widened implying that the particle size is very small according to the Debye–Scherrer formula D=Kλ/(βcosθ), where K is the Scherrer constant, λ the X-ray wavelength, β the peak width of half-maximum, and θ is the Bragg diffraction angle [23].
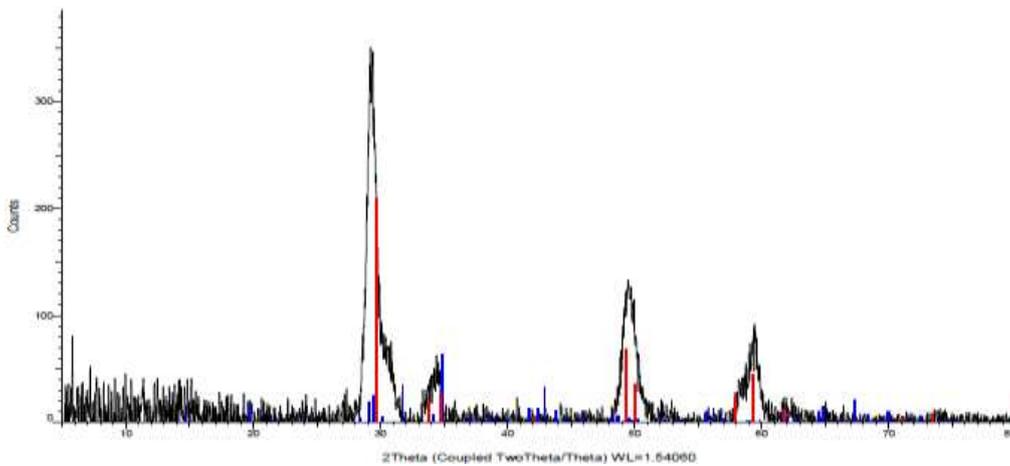
Fig. 5. XRD spectrum of Al_2O_3-ZrO_2 nanocomposite.

Red peaks are for ZrO_2 and blue peaks are for Al_2O_3. The repeated peaks in the red could be associated with the reflection of the same structure. This observation is in full agreement with TEM results revealing the composite structure of the sample which consists of nanometer scale reinforcement (<6nm) in the similar size (<50nm) matrix. Based on the XRD spectrum, the structure of the sample seems to be uniformly ordered, however TEM images visualize the irregular/ random shapes of the particles. Calcination at 900^0C results in crystallization and morphology of the nanocomposite displaying numerous narrow peaks assigned to the whole set of reflection characteristics for the regular structure of Al_2O_3.

IV. Mechanical Properties

The Halpin-Tsai equations [24, 25] use the mechanical properties of the fiber and the matrix to calculate the properties of the composite. This model assumes an isotropic particulate reinforcement of the matrix. The following relations are used to evaluate the property;

$$P = P_m \frac{(1+\varphi e_P v_f)}{(1-ev_f)} \qquad (1)$$

where;

$$e_P = \frac{(P_f - P_m)}{(P_f + \varphi P_m)} \qquad (2)$$

$$\varphi = \left[2 + \left(40 * v_f\right)\right] \tag{3}$$

In the above Equations (1)-(3) *P* stands for a property such as density, modulus of elasticity, Poisson's ratio etc. and suffixes *m* and *f* corresponds to matrix and filler respectively. The term e_P is a factor corresponding to a property which depends on another factor φ also varying with volume fraction of the filler. The mechanical properties of nanocomposite particles are evaluated by using the above mentioned approach. Individual characteristics of Al_2O_3 and ZrO_2 are extracted from the literature and tabulated in the Table 1. The respective properties of Al_2O_3-ZrO_2 nanoparticles reported by this study (5% reinforcement) are illustrated in the Figs. 6-8. A MATLAB script is written to plot the trend of these characteristics with the variation in the volume fraction of nanoparticles and illustrated in the following Figs.

Table 1. Mechanical Properties of Al_2O_3 and ZrO_2. The properties reported by previous researchers are taken as references [26, 27].

Sr. No.	Properties and notations used	Unit	Alumina (Al_2O_3)	Zirconia (ZrO_2)	(Al_2O_3-ZrO_2) Nanocomposite (5% by Vol.)	
					By this study	From Literature
1	Density (ρ)	Kg/m^3	3900	6000	3995.23	4100
2	Tensile Strength (σ_T)	MPa	480	1100	504.85	----
3	Hardness (Vickers)	VPN	2000	1300	1962.64	1750
4	Flexural Strength	MPa	379	900	399.69	760
5	Elastic Modulus (E)	GPa	370	205	361	310
6	Shear Modulus (G)	GPa	152	80	148.03	----
7	Thermal Conductivity (λ)	W/mK	35	2	33	23
8	Fracture Toughness	MPa-m$^{1/2}$	4	13	4.31	6
9	Poisson's Ratio (ν)	No unit	0.22	0.31	0.224	0.23

The microstructure of ZTA consists of alumina matrix containing dispersed particles of zirconia. The mechanical properties of nanocomposite can be significantly improved via two different mechanisms: microcracking and stress induced transformation toughening. Microcracks are induced by the volume change of ZrO_2 phase during sintering and calcination, when cooled through the transformation temperature. Tangential stresses are generated around the transformed particle that induces microcracks in the matrix. The cracks have the ability to absorb or dissipate the energy, thereby increasing the toughness of the composite. Stress-induced transformation toughening is caused by tetragonal zirconia particles when interacting with an advancing crack which then promote a toughening effect through the permanent dilatation and reduced modulus that they imply around the crack-tip. Since the strain occurs in the vicinity of the crack; extra work would be required to move the crack through the ceramic, accounting for the increase in toughness and strength [28, 29]. The hardness of the ZTA composite decreases as alumina is harder than zirconia. The difference in the coefficient of thermal expansion between the matrix and the dispersed phases causes the reduction in thermal conductivity of the composite. The modulus of elasticity of the composite depends on the volume fraction of the phases present and their individual modulii. Elastic modulus of alumina is greater than that of zirconia, hence the addition of zirconia affects adversely on modulus of the composite.
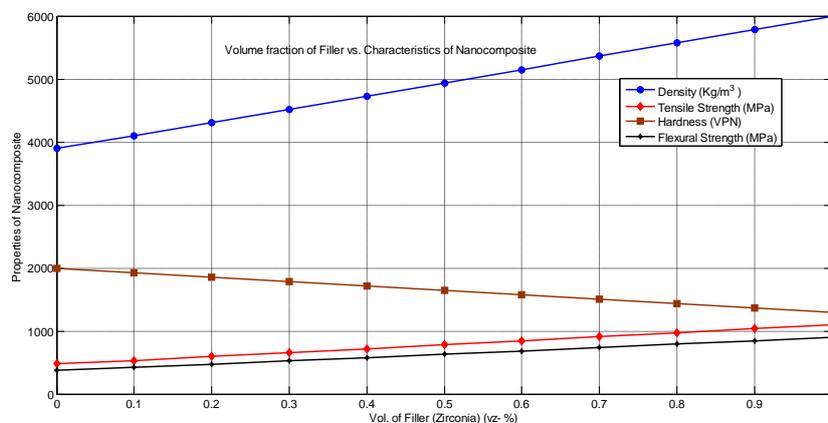
Fig. 6. Mechanical Properties of Al_2O_3-ZrO_2 nanocomposite. Density, Tensile Strength and Flexural Strength increases, whereas Hardness decreases.
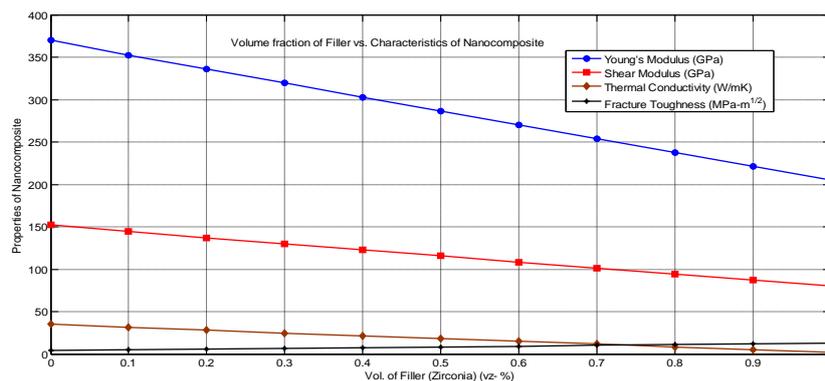
Fig. 7. Mechanical Properties of Al_2O_3-ZrO_2 nanocomposite. Fracture Toughness increases, whereas Modulii and Thermal Conductivity decreases.
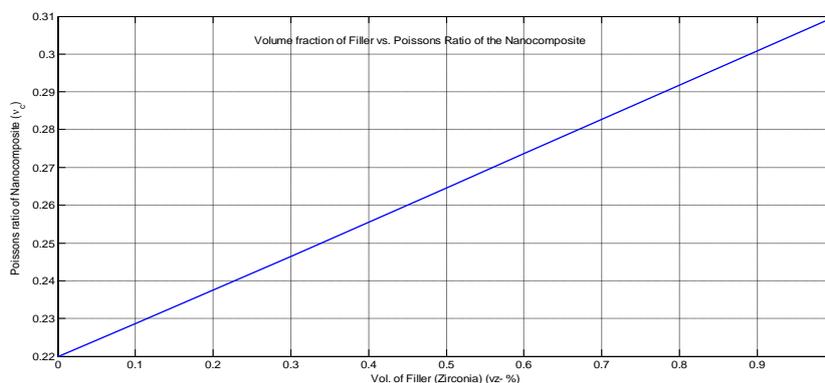
Fig. 8. Mechanical Properties of Al_2O_3-ZrO_2 nanocomposite. Poisson's Ratio directly increases with increase in volume fraction of nanofillers.

V. Microsystem Interaction

The results of this study provide a clear evidence for the complexity of the structural genesis of binary ZrO_2 into ternary Al_2O_3 oxides. It exists from an amorphous solid precursor ($Al(NO_3)_3$ and $ZrOCl_2$) through assembling of nanosized crystallites during sol-gel processing up to a final well-crystalline compound. Interestingly, a remarkable point is that the transformation of the chloride and nitrous precursor from a nanostructural state into a regular nanocomposite structure occurs in a fairly narrow temperature interval at ambient temperature. The nanocomposite structure described as a network built up of tetragonal ZrO_2 with lattice parameters a=b= 7.28818Å, c= 5.30143 Å and α=β=γ= 90^0 in orthorhombic Al_2O_3 matrix with lattice parameters a= 4.84350 Å, b= 8.22240 Å, c= 9.00110 Å. Though the structure of the complex Al_2O_3- ZrO_2 compound has not been determined yet, this study may provide some suggestions concerning the distribution of the Zr doping ions in the Al-oxide structure. Zr^{4+} ions have been found in octahedral coordination characteristic for Al^{3+} ions. Since the structure of Al_2O_3- ZrO_2 is based on slabs of octahedrons occupied by Al^{3+} ions, these positions might be, therefore, partially occupied by Zr^{4+} ions. The lateral growth of ZrO_2 slabs inside the Al_2O_3 is controlled by diffusional migration of the O^{2-} ions. The nucleation and growth of triclinic ZrO_2 cell is controlled by the rapid and diffusionless shear displacement of the Zr^{4+} ions. The orientation of the Zr^{4+} and O^{2-} ions to their respective positions are controlled by the diffusional displacement of the respective ions, transformation temperature and time [27]. At the same time, FTIR spectrum delivers certain hints on the presence of Zr^{4+} ions in an uncommon, maybe highly distorted trigonal pyramidal coordination. We may speculate that these ions substitute Al^{3+} ions in orthorhombic bipyramidal sites. It is to be noted that the analogies exist in the preferred coordination of Al^{3+} and Zr^{4+} ions.

VI. Conclusion

Sol-gel process is found to be an effective route to form alumina-zirconia nanocomposite particles with control over size, distribution and morphology of the compound. TEM and SEM micrographs verify the microstructural details, nanometer size and reinforced features of secondary phase in the ceramic matrix which is also validated by IR spectroscopy and X-ray Diffractometry. The physical and mechanical properties of the composite are found to be a function of dispersed zirconia particle size and could be mentioned as below:
1.   Hardness decreases with the addition of zirconia as alumina is much harder than zirconia.
2.   Tensile strength and flexural strength increases linearly with volume fraction of zirconia.

3. The fracture toughness also increases due to microcrack formation at the orientation of zirconia particles, but the stiffness decreases reducing the elastic and shear modulii.
4. Density and Poisson's ratio are in direct proportion with volume fraction of zirconia.

Acknowledgement

References

[1]. H. Farzana, H. Mehdi, and O. Masami et al. Review article: Polymer-matrix nanocomposites, processing, manufacturing, and application: An overview, Journal of Composite Materials, 40(17), 2006, 1511-1575.
[2]. K. Niihara, New design concept of structural ceramics-ceramic nanocomposite, Journal of Ceramic Society of Japan, 99(10), 1991, 974-982.
[3]. S. Komarneni, Nanocomposites, Journal of Materials Chemistry, 2(12), 1992, 1219-1230.
[4]. A. Borrell, V.G. Rocha, and R. Torrecillas et al. Effect of carbon nanofibers content on thermal properties of ceramic nanocomposites, Journal of Composite Materials, 46(10), 2012, 1229-1234.
[5]. K.S. Tun, and M. Gupta, Role of Microstructure and Texture on Compressive Strength Improvement of $Mg/(Y_2O_3 + Cu)$ Hybrid Nanocomposites, Journal of Composite Materials, 44(25), 2010, 3033-3050.
[6]. E. Dorre and H. Hubner, Alumina (New York: Springer-Verlag, 1984).
[7]. A. Thirunavukkarasu, S.K. Malhotra, and S. Paramanand, High Toughness Alumina – Zirconia Nanocomposites from Sol gel Nanopowders, Int Symp of Research Students on Material Science and Engineering, Chennai, India, 2004, 1-9.
[8]. B. Basu, T. Venkateswaran, D. Sarkar, Pressureless sintering and tribological properties of WC–ZrO2 composites. Journal of European Ceramic Society, 25 (9), 2005, 1603–1610.
[9]. R.H.J. Hannink, and M.V. Swain, Progress in transformation toughening of ceramics, Annual Review of Material Science, 24, 1994, 359–408.
[10]. S. Kobayashi, and S. Wada, Strengthening of Si_3N_4 Ceramics by ZrO_2 additions, Advances In Ceramics, 24A, 1998, 127-132.
[11]. B. Kerkwijk, A.J.A. Winnubst, and H. Verweij et al. Tribological properties of nanoscale alumina–zirconia composites, Wear, 225, 1999, 1293–1302.
[12]. J.M. Tang, M. Uehara, and H. Maeda et al. Process study on alumina-zirconia nanocomposite via ammonolysis route, Journal of Ceramic Processing and Research, 1(2), 2000, 88-91.
[13]. R. Guo, D. Guo, and D. Zhao et al. Low temperature ageing in water vapor and mechanical properties of ZTA ceramics, Materials Letters, 56, 2002, 1014–1018.
[14]. H. Antonio, D. Aza, and J. Chevalier et al. Slow-crack- growth behavior of Zirconia-toughened Alumina ceramics processed by different methods, Journal of American Ceramic Society, 86 (1), 2003, 115–120.
[15]. X.W. Huang, S.W. Wang, and X.X. Huang, Microstructure and mechanical properties of ZTA fabricated by liquid phase sintering, Ceramics International, 29, 2003, 765–769.
[16]. D. Casellas, M.M. Nagl, and L. Llanes et al. Fracture toughness of alumina and ZTA ceramics: microstructural coarsening effects, Journal of Materials Processing Technology, 143–144, 2003, 148–152.
[17]. A.P. Quintina, M.H. Bergera, and A.R. Bunsella et al. Processing and structures of bi-phase oxide ceramic filaments, Journal of European Ceramic Society, 24, 2004, 101–110.
[18]. A. Dakskobler, and T. Kosmac, The preparation and properties of Al_2O_3–ZrO_2 composites with corrugated microstructures, Journal of European Ceramic Society, 24, 2004, 3351–3357.
[19]. S.T. Aruna, and K.S. Rajam, Mixture of fuels approach for the solution combustion synthesis of Al_2O_3–ZrO_2 nanocomposite, Materials Research Bulletin, 39, 2004, 157–167.
[20]. D. Sarkar, S. Adak, and N.K. Mitra, Preparation and characterization of an Al_2O_3–ZrO_2 nanocomposite, Part I: Powder synthesis and transformation behavior during fracture, Composites A: Applied Science and Manufacturing, 38(1), 2007,124-131.
[21]. S.J. Mousavi, S.M. Hosseini, and M.R. Abolhassani et al. Calculation of the structural, electrical, and optical properties of $ƙ$-Al_2O_3 by density functional theory, Chinese Journal of Physics, 46(2), 2008, 170-180.
[22]. M. Yashima, Crystal structures of the tetragonal Ceria− Zirconia solid solutions Ce x Zr1− x O2 through first principles calculations (0≤ x≤ 1), Journal of Physical Chemistry C, 113(29), 2009, 12658-12662.
[23]. R.Y. Hong, J.H. Li, and L.L. Chen LL et al. Synthesis, surface modification and photocatalytic property of ZnO nanoparticles, Powder Technology, 189, 2009, 426–432.
[24]. J.E. Ashton, J.C. Halpin, and P.H. Petit, Primer on composite materials: Analysis. (Stamford: Technomic Pub., 1969).
[25]. J.C. Halpin, Stiffness and expansion estimates for oriented short fiber composites. Journal of Composite Materials, 3, 1969, 732-734.
[26]. http://accuratus.com/zirc.html (Accessed on 03 Sept, 2013 at 04:16 p.m. IST.)
[27]. D. Sarkar, Synthesis and thermo-mechanical properties of sol-gel derived Zirconia toughened Alumina nanocomposite, doctoral diss., NIT Rourkela, India, 2007.
[28]. F.F. Lange, B.I. Davies, and D.O. Raleigh, Transformation strengthening of β"-Al_2O_3 with tetragonal ZrO_2. Journal of American Ceramic Society, 66 C, 1983, 125-127.
[29]. R. Stevens, Zirconia and Zirconia Ceramics, (Magnesium Elektron, 1986).